Theoretical and experimental study of the graphite 1*s* x-ray absorption edges

R. Ahuja and P. A. Brühwiler
Department of Physics, Uppsala University, Box 530, S-751 21 Uppsala, Sweden

J. M. Wills
Theoretical Division, Los Alamos National Laboratory, Los Alamos, New Mexico 87544

B. Johansson, N. Mårtensson, and O. Eriksson
Department of Physics, Uppsala University, Box 530, S-751 21 Uppsala, Sweden

(Received 20 May 1996)

Theoretical calculations in combination with experiments for the π^* and σ^* x-ray absorption edges are reported for graphite. Theory and experiment agree well for the leading π^* and σ^* resonances. By comparing theoretical calculations for a single graphene layer that include the effect of the core hole to similar calculations that do not, we find that 1*s* x-ray absorption in graphite is to be associated with an excitonic effect. Both the π^* and σ^* excitons are localized primarily on the core-excited atom, but have significant weight on the nearest-neighbor atoms. The results are closely related to the electronic structure of a N impurity. [S0163-1829(96)01044-2]

I. INTRODUCTION

Graphite can be regarded as a prototype of layered crystals. The crystal structure is hexagonal with four atoms per unit cell, arranged as a group of weakly interacting hexagonal planes. The carbon atoms in the basal plane are bound together by strong covalent bonds while the atoms in the adjacent planes are weakly bound by van der Waals forces. Thus, the interlayer nearest-neighbor distance (3.35 Å) is much larger than the in-plane nearest-neighbor distance (1.42 Å). The bonding properties of graphite can be explained by so-called sp^2 hybrids, which are orbitals that point in the direction of the neighboring atoms. Three of the four valence electrons are assigned to these trigonally directed orbitals, which form σ bonds. The fourth electron lies in the p_z orbital, which is oriented normal to the σ-bonding plane and forms weaker π bonds. As a result of the unusual bonding properties one can describe the main features of the electronic structure of graphite by considering only one sheet of carbon atoms (graphene).

The unusual structural properties of this material are expected to result in unique electronic structure-related properties. This has motivated several investigators to calculate the energy band structure and related properties. One of the earlier theoretical attempts made use of the so-called $\mathbf{k}\cdot\mathbf{p}$ method, and the energy bands near the Fermi level (E_F) were described by seven parameters.[1,2] The electronic structure of graphite has also been calculated self-consistently by means of the local density approximation (LDA), using different computational methods such as the linear combination of atomic orbitals method,[3] the Korringa-Kohn-Rostoker method,[4] the full-potential linearized augmented plane wave method,[5,6] the pseudopotential method,[7–9] and the full-potential linear muffin-tin-orbitals (FPLMTO) method.[10]

Our interest here is to use such techniques in combination with experimental data to understand the effect of a 1*s* hole on the electronic structure of graphite. Core level techniques used to study the graphite electronic states include x-ray absorption (XAS),[11–17] photoelectron (XPS),[18–20] Auger,[21,22] x-ray emission (XES),[15,16,23–25] resonant inelastic x-ray scattering (RIXS),[16,25] and autoionization[17] spectroscopies. Various properties have been derived from these spectra, but of central interest for this work is the nature of the π^* and σ^* thresholds measured by XAS.[11,12,14–17] Concerning this issue Mele and Ritsko considered[11] a single layer of graphite in a tight-binding method and calculated both the ground-state density of states (DOS) as well as the DOS in the presence of a core hole. Their study showed that the ground-state DOS had a peak 3 eV above E_F, compared with the XAS spectra which show the peak 1 eV above threshold. The agreement between experiment and theory was improved when considering the DOS in the presence of a core hole. In this calculation the peak position moved down $\sim$2 eV. Mele and Ritsko concluded that the peak in the XAS spectrum is to be associated with an (Frenkel) excitonic effect. This conclusion was contradicted by Weng *et al.*,[26] who argued that the ground-state DOS accurately models the XAS spectrum, and whose arguments were used to explain newer experimental data.[14] Recent multiple scattering calculations give support to the results of Weng *et al.*,[27] whereas a recent perturbation theoretical treatment of XAS and inelastic x-ray scattering used the assumption that core-hole effects were important, with reasonable success,[28] but came to no conclusions about the relative accuracy in describing experimental data after including core-hole effects. More recently another experimental probe, core level autoionization,[17] has given evidence that the original conclusion of Mele and Ritsko is correct, i.e., that the π^* threshold in graphite is strongly affected by excitonic effects.

The σ^* threshold has also been the subject of recent discussions.[26,14,15] Again, the controversy concerns the role of the core hole in the character of the excited state. Weng *et al.* and Batson maintained that the ground-state calculation served well to explain the threshold region, whereas Ma

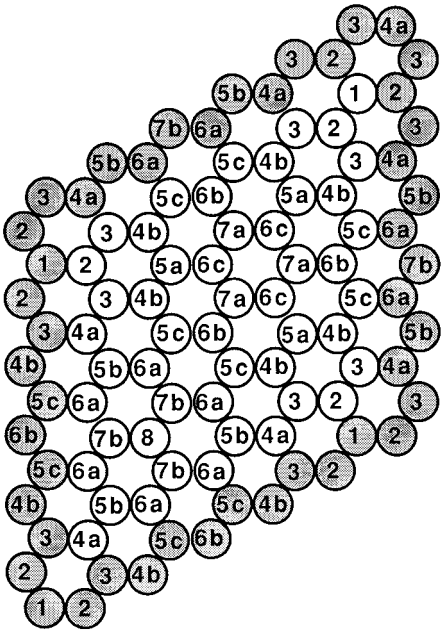

FIG. 1. Supercell used in the calculations. The core-excited atom is at location 1, and the higher numbers indicate the distance from a core-hole site.

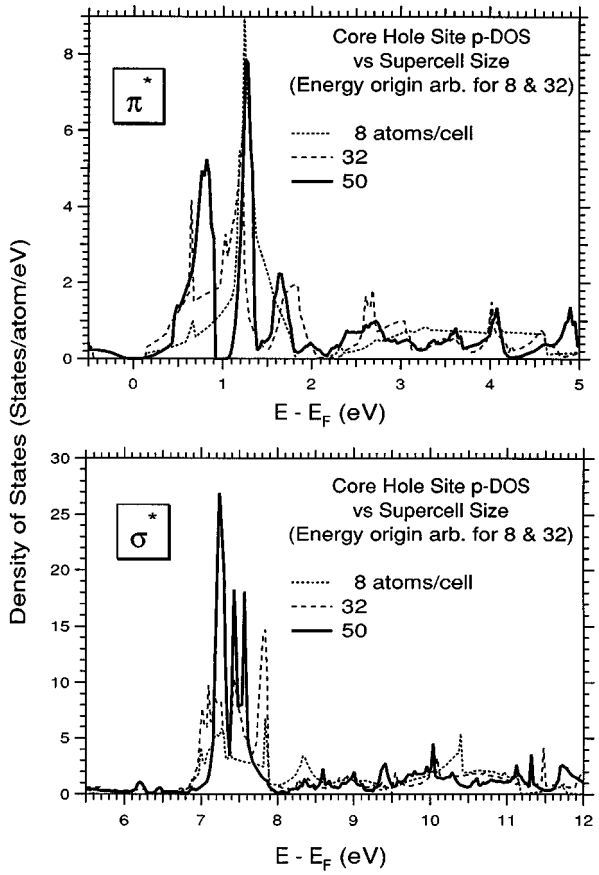

FIG. 2. Excited-state DOS at the core-hole site as a function of the size of the supercell used in the calculations. As seen in Fig. 1, the distance between core-hole sites for a 50-atom cell is 10 bonds. For the 32-atom case, it is 8 bonds, and for the 8-atom case, 4 bonds.

et al. presented XES data which suggested that the first σ^* peak has excitonic character.[15] This latter finding was supported by Brühwiler *et al.*[17]

The above-mentioned controversies of how to interpret the XAS spectrum in graphite (excitonic effects or not) have motivated us to extend the theoretical study of the threshold region in graphite. The different conclusions in the previous investigations may be due to differences in the different experimental spectra and/or differences in the quality of the theoretical work. Therefore we have performed theoretical calculations for the XAS spectrum of graphite, to compare the calculated core-excited DOS to the experimental data. We also analyze the spatial extent of the changes in the DOS induced by a core hole, and compare it to related work on other sp-bonded systems.

II. DETAILS OF THE CALCULATIONS

In our present calculations we used a FPLMTO technique.[29] The calculations were all electron and scalar relativistic. The charge density and potential were allowed to have any shape inside the muffin tins as well as in the interstitial region. The basis set, charge density, and potential were expanded in spherical harmonic series (with a cutoff $l_{\max}=6$) within the nonoverlaping muffin-tin spheres (the muffin-tin radius was 1.25 a.u. in the calculations) and in a Fourier series in the interstitial region. The basis set was comprised of augmented linear muffin-tin orbitals.[30,31] The tails of the basis functions outside their parent spheres were linear combinations of Hankel or Neuman functions with nonzero kinetic energy.

In order to simulate a system with a core hole excited, we performed calculations in a supercell geometry, shown in Fig. 1. For one of the atoms in the cell (atom 1) we omitted one of the electrons in the 1s orbital, whereas the number of electrons in the valence band was increased by one. This procedure simulates the experimental situation, in which the sample can easily supply an electron to screen a localized charge. The supercell in Fig. 1 is repeated periodially both in the xy plane as well as along the z axis, so that we maintain periodic boundary conditions. The distance between the graphene planes was kept large in order to prevent layer-layer interaction. In order to make sure that the different core-excited atoms are sufficiently isolated in our model we have perfomed test calculations with increasing cell sizes, going up to a maximum of 50 atoms in a graphene plane. The calculated properties of the core-hole-excited system are found to be converged for a 50-atom cell, as indicated in Fig. 2. One should note here that the π^* peak seems to converge faster with respect to supercell size compared to the σ^* peak. We have also investigated the convergence of the supercell size with respect to stacking of atomic planes along the c axis. To do this we compared calculated spectra with every graphene plane containing a core-hole superstructure to calculations where every other graphene plane was unexcited. The two calculations gave very similar results, suggesting that the interactions between the planes is small, so that we can approximate the experimental process by considering a core-hole superstructure in every plane. This greatly reduces the size of the calculational effort.

The isolation of the impurity site in our calculations is

comparable to that found to closely mimic the isolated impurity in first-principles supercell calculations for diamond.[32] We note that semiempirical calculations of the charge density induced by a N impurity in graphite suggested that a cell of 18 atoms did well to describe the local effects, but even a cell of 53 atoms did not take full account of the long-range Friedel oscillations.[33]

The integration over the Brillouin zone was done using a special point sampling[34] with a Gaussian smearing of 20 mRy using 28 k points in 1/12 of the Brillouin zone. The calculations were done at the experimental lattice constant, and the ratio between the interstitial region and unit cell volumes was approximately 0.1. The potential was calculated using the LDA with the Hedin-Lundqvist[35] expression for the exchange and correlation potential.

Throughout our analysis of the self-consistent calculations we determined the Fermi level having four valence electrons per carbon atom plus one extra (screening) electron as described above. However, when we compare our calculated spectra with measured XAS data we aligned the theoretical spectra so that the semimetallic minimum in the DOS of an atom far away from the core-hole atom coincided with the experimental Fermi level. This corresponds most closely to the experimental situation where E_F is situated in a semimetallic region for an atom far away from the core-excited atom.

As a last comment on the calculational details we note that our approach is short of the full calculation needed to determine the relative energies of excited states above the edge, which would require a quasiparticle treatment[36,25] in order to account for the screening of the promoted electron. However, these effects are minor, as discussed below. Thus, the present calculations serve to isolate the major effects of the core hole.

III. EXPERIMENTAL DETAILS

The XAS data were taken at Beamline 22 at MAX-Lab in Lund using partial yield and a photon energy resolution of 0.13 eV, as described previously.[17] They have been corrected for variations in the beamline throughput with photon energy, and are in agreement with previous results,[11–16] especially the most recent high-resolution work.[13–16] The line shape at the σ^* edge represents the most stringent test of experimental resolution in these data, and our data are among the best resolved.

The calibration of the energy scale is vital for the present comparison of data and theory. This was accomplished for the photon energy by taking the kinetic energy difference of the Pt $4f$ photoemission lines excited by first- and second-order light (tuned to the threshold of 284.4 eV), using a Pt(111) crystal which was in electrical contact with the graphite sample. The reference energy for the threshold, which is the C $1s$ binding energy,[17] was determined via reference to E_F of the same Pt crystal, since the DOS is very low at E_F for graphite. It is the C $1s$ binding energy which is subtracted from the photon energy to make the comparisons between theory and experiment in the figures which follow.

IV. THEORETICAL RESULTS

In support of previous model calculations,[11,26,37] we obtain from the ground-state DOS calculation (no core hole) a

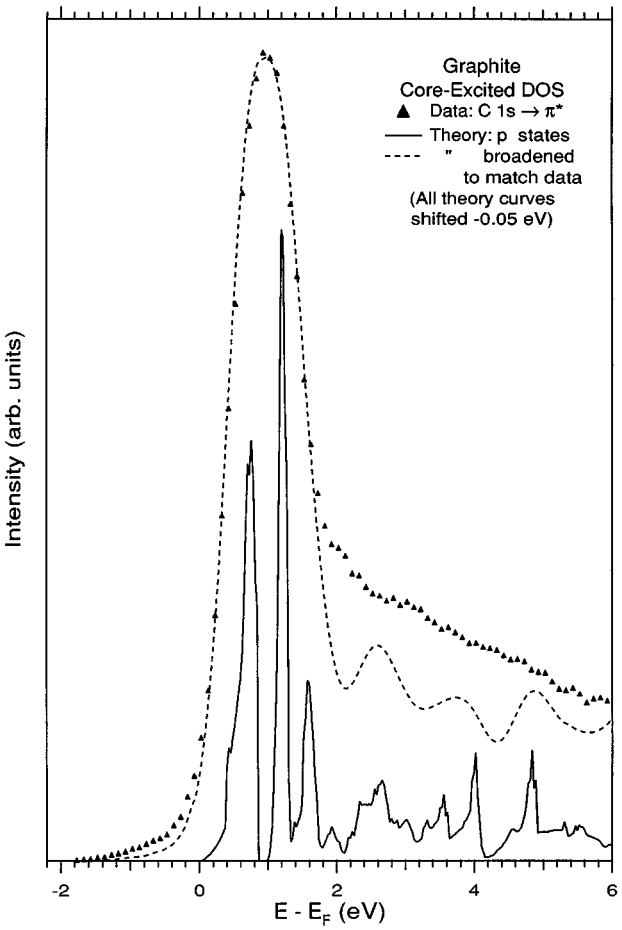

FIG. 3. Comparison of XAS data and theory of graphite. The data were taken with light polarized in the plane of incidence, incident at 75° with respect to normal, emphasizing the π^* states.

π^* peak which is broader than the experimental data as well as situated too high above the threshold. In the DOS calculation of Mele and Ritsko the peak was found at 3 eV, whereas we find it at 2 eV. This is quite close to a recent quasiparticle calculation for the graphite band structure, based on the location of the saddle point in the band dispersion from $\Gamma-M-K$,[25] suggesting that quasiparticle self-energies are small at this energy in agreement with recent measurements.[38] However, the alignment between experiment and theory is still far from satisfying.

In contrast, the calculation which accounts for the core hole yields a spectrum which is quite similar to experiment in position and shape of the large π^* resonance, shown in Fig. 3 together with experiment. To achieve this level of agreement in the line shape, we have broadened the calculated DOS by a Voigt function encompassing a 0.10 eV Lorentzian contribution to account for the core-hole lifetime,[17,39,40] and a Gaussian contribution of 0.6 eV to account for vibrational and resolution broadening, and shifted the theoretical curves downward in energy by 0.05 eV, which is at the limit of the experimental uncertainty. The vibrational contribution to the dashed line in Fig. 3 is also 0.6 eV, since the photon energy resolution of 0.13 eV is very small in comparison to the broadening required to match theory to experiment. As seen in Fig. 2, this width is supercell-size independent. The broadening is quite compa-

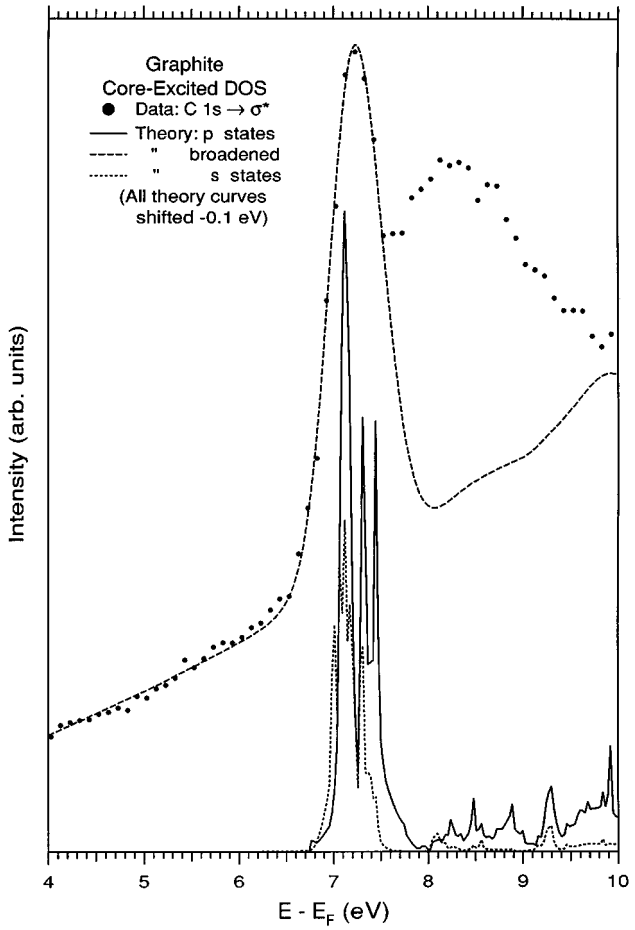

FIG. 4. Comparison of XAS data and theory of graphite, the latter broadened and with a linear background added to match the data. The data were taken at normal incidence, emphasizing the σ^* states.

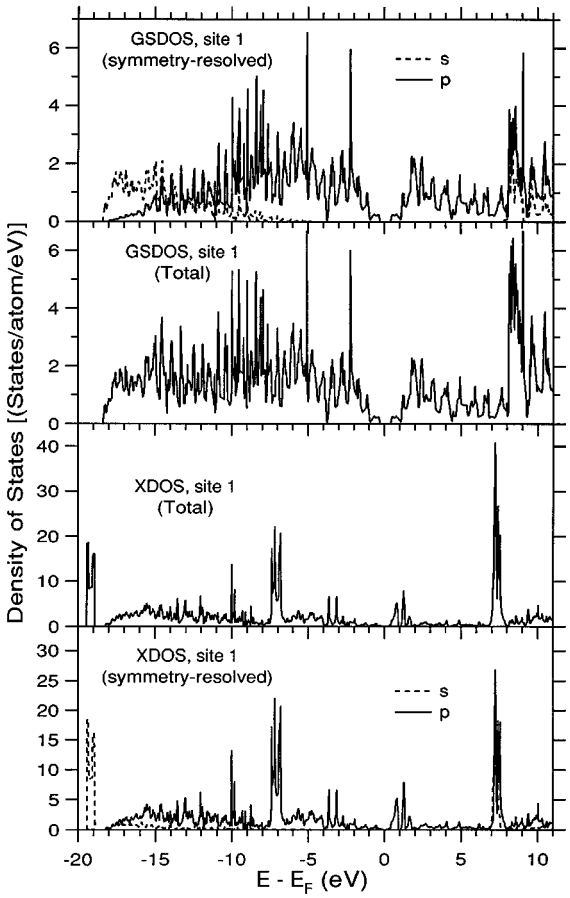

FIG. 5. Calculated DOS for site 1 (see Fig. 1) with and without a core hole, and total and symmetry resolved, taking account only of states within the muffin-tin sphere.

rable to that found, e.g., for benzene in the gas phase,[41] and slightly larger than that found[39] for C_{60}, suggesting that this is a reasonable estimate of the true phonon broadening. We note here that the DOS curve in Fig. 3 (and in the subsequent DOS plots) represents electronic states projected inside the muffin-tin sphere. We are thus neglecting the interstitial contribution. However, this contribution to the XAS model calculation is very small, since the core state which would enter the matrix elements has almost no weight in this spatial region.

In Fig. 4 we compare the experimental and theoretical data for the σ^* resonance. In this figure we have employed a -0.10 eV shift of the theoretical curve, and have broadened the data using a Voigt function encompassing the same 0.1 eV Lorentzian lifetime contribution used for the π^* resonance, with a 0.2 eV Gaussian. This latter amounts to 0.16 eV unexplained broadening, which we attribute to phonons. Thus, the broadening determined in this way is much less than that found at the π^* resonance. We note that theory and experiment agree on the position of the sharp resonance. However, the broader hump above the first resonance is not reproduced. Another notable point is that there *are* bands which account for a low DOS of σ^* symmetry below the σ^* edge, based on ground state[10] and quasiparticle[25] calculations. However, no states of such symmetry appear below the σ^* edge in our calculations when a core hole is included.

In Fig. 5 we show the partial and total DOS projected on the muffin-tin site surrounding the core-hole-excited atom. We will loosely refer to these curves as the excited-state DOS (XDOS). We present for comparison the corresponding ground-state DOS (GSDOS) as well. The GSDOS was calculated from a single layer 50 atom supercell in order to make a comparison with the XDOS clearer. The GSDOS thus does not quite resemble the GSDOS of three dimensional graphite, as may, for instance, be seen in the small band gap, a feature which is replaced by semimetallic behavior in bulk graphite. When comparing the GSDOS and XDOS we note that the presence of the core-hole induces large modifications of the theoretical electronic states. As mentioned earlier, the peak just above E_F in the GSDOS is lowered in energy and narrows in the XDOS, with a good correspondence to XAS spectra (Fig. 3). There is no arbitrary shifting involved to obtain this good agreement, since E_F was determined for the experimental data in Fig. 3 using[17] the C 1*s* binding energy. Moreover, the σ^* peak at $E_F+8.5$ eV in the GSDOS curve is lowered to $E_F+7.3$ eV in the XDOS curve, and as mentioned this is also in good agreement with experiment. Also, at E_F-7 eV a rather sharp feature appears in the XDOS and a single, narrow band is split off at E_F-19 eV. This latter feature is composed mainly of states of *s* character, whereas all the other peaks

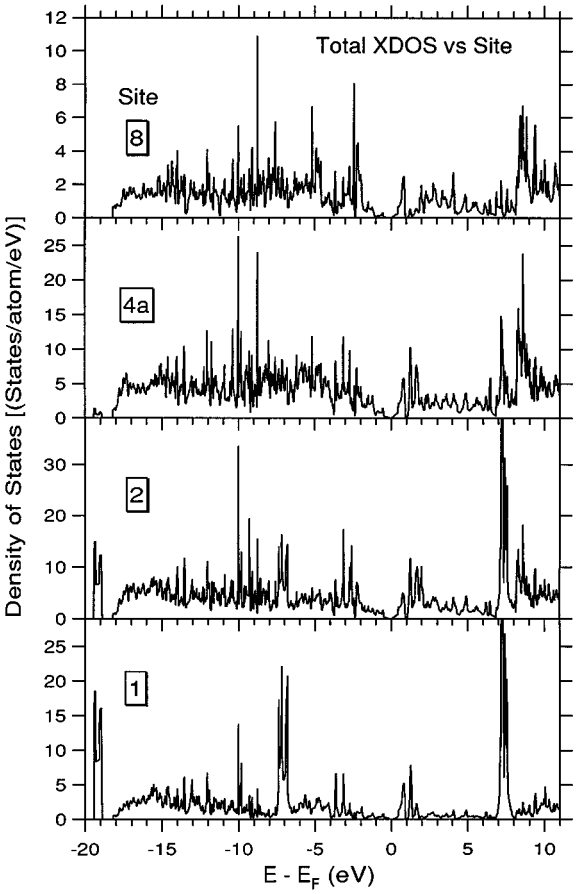

FIG. 6. Local XDOS at selected atomic sites in the supercell. The core-excited atom is at location 1, and the higher numbers give a measure of distance from the core-hole site as seen in Fig. 1. See Fig. 5 for more details on the local XDOS at location 1.

mentioned above are dominated by the p orbitals.

In Fig. 6 we present the XDOS projected on the different atoms in the supercell. The largest modification of the XDOS is found for the atom which has a core hole (atom 1). However, for some of the other atoms in the cell there is also a redistribution of the electronic states. For instance, the nearest-neighbor atom has an XDOS which resembles that of the core-hole-excited atom, albeit with less pronounced features. As an example we note that atom 2 also has a peak at E_F-19 eV. Thus the single s state which is split off at low energies has its main weight on the core-excited atom, but also has weight at the nearest-neighbor atoms. The presence of a core hole apparently modifies the s orbitals from being quite broad states which contribute to the formation of the bonding sp^2 orbitals, to a localized state which has wave-function character mostly projected on the central atom and only partly on the nearest neighbor. One can view this process as follows: the presence of a core hole on the central atom lowers the energy of the s orbital so that, in the language of Harrison's analysis[42] of the chemical bonding in these materials, the formation of an sp^2 bond orbital is energetically unfavorable. The overlap between the s wave functions is also reduced due to the accompanying contraction of the s orbital, and as a result of these two effects an almost localized level at E_F-19 eV develops. In a similar way we find that the features at E_F-7 eV, E_F+1 eV, and at

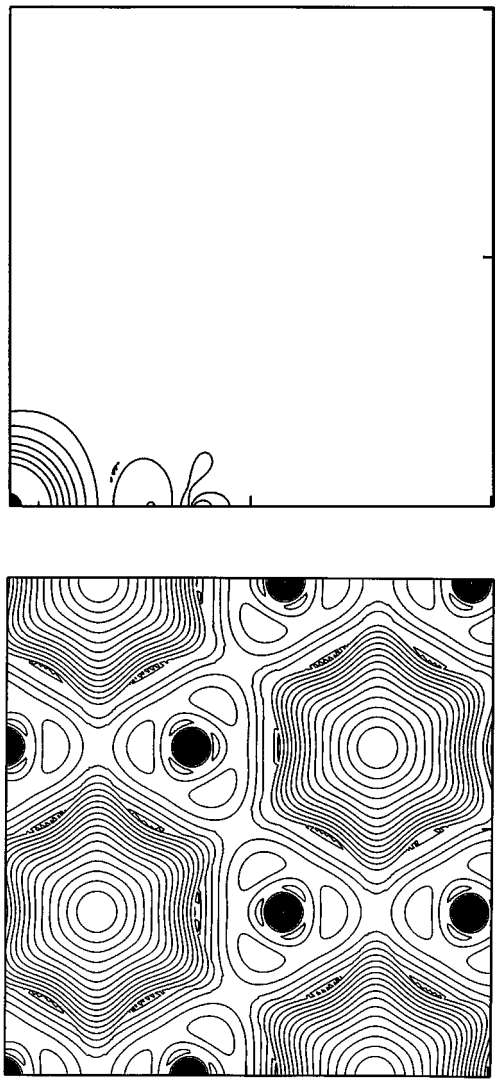

FIG. 7. Lower figure: charge density contours for the ground-state graphite monolayer. Upper figure: changes in charge density in the region of the core hole, which is located at the lower left corner.

$E_F+7.3$ eV in the XDOS curve mainly originate from states on the core-hole-excited atom, but there is some weight of these states on the nearest neighbors.

Consistent with the analysis above, i.e., that most of the modification of the XDOS curves is found for the core-excited atom, we find that the dominant part of the screening charge which accompanies the core hole accumulates inside the muffin-tin sphere of the core-excited atom. In Fig. 7, we show the density distribution of the screening charge (upper figure) and compare it with the total ground-state valence charge density of graphite (lower figure). The core-hole-excited atom is situated at the lower left corner of the figure. Note that the charge density of graphite follows what is expected from sp^2 bonding, with lobes of charge pointing in the direction of the nearest-neighboring atoms (see lower figure). The screening charge is mostly localized on the core-excited atom, and the screening charge density is dominated by a spherical contribution. However, it is interesting to note that there is a modification of the charge density also on the nearest neighbors of the core-excited atom. On these atoms the screening charge is negative and nonspherical. Thus the

nonspherical regions on the x axis represent a depletion of charge as does the nonspherical region on the y axis. This means that in the excited state the core-excited atom attracts charge from the nearest neighbors, in order to screen the core hole. A similar pattern has been observed in calculations of core-hole screening in C_{60}.[43]

V. DISCUSSION

A. π^* excitation

1. Comparison with previous calculations

The results above agree with previous work on the charge distribution of a N impurity in graphite.[44,33] Furthermore, the localization of the screening found in the present analysis is in line with the previous interpretation of XAS spectra, i.e., the x-ray absorption in graphite is to be associated with an (Frenkel) excitonic effect. Upon comparing our results with the model calculation of Mele and Ritsko, we conclude that the present study is in better agreement with experiment. Since the theoretically determined width of the graphite π^* resonance does not increase with supercell size, it seems most likely that the experimentally observed width is indeed dominated by vibrational coupling. Experiment does not give much useful input into this question: the intensities of the resonant photoemission like parts of the spectra, which as explained earlier[45] can be related to resonance widths, are highly dependent on questions of matrix elements, which have been shown to vary, e.g., for C_{60}, depending on the core-excited states studied.[46] Already it can be seen from Figs. 2 and 3 of Ref. 17 that such effects are almost certainly occurring, since using the normalization given there to compare to the Auger, the difference between autoionization and Auger at the π^* threshold is positive across the width of the spectra, but has negative excursions for autoionization at the σ^* threshold.[45] Understanding these quantitative discrepancies awaits future improvements, on both the experimental and theoretical fronts. We conclude that the difference between our theoretical results and those of Ref. 11 is likely due to the differences in the computational techniques, since the pioneering calculation of Mele and Ritsko was based on model parameters, whereas the present calculations are *ab initio*, and rely on very few approximations. Primarily, the differences can be ascribed to the conclusion above that the vibrational broadening is found to greatly affect the overall linewidth, and the latter was accounted for purely via electronic effects in the earlier work.

An interesting finding, shown in Fig. 3, is that the unbroadened theoretical XAS π^* resonance is composed of two well-separated peaks. There is also an additional smaller peak at $E_F+1.5$ eV. In the broadened spectrum these peaks merge into one, but it is of interest to try to understand why the presense of a core hole not only moves down and narrows the π^* bands, but also splits them into several features. In analogy with the Andersen impurity model one may explain the shape of the π^* resonance as originating from two bands which hybridize. Before considering hybridization one band is a dispersionless p_z band which has its origin from the core-hole-excited atoms. In our supercell, core-hole-excited atoms have very little overlap, and thus in the absence of hybridization with other states the p_z states on the core-hole-excited atoms give rise to states which have very little dispersion. The other band is a π^* band, which originates from atoms which do not have a core hole excited and this band has dispersion. The two bands are located in the same energy region (0–2 eV above E_F) and thus we have one band which displays dispersion intercepted by a dispersionless level. If one now turns on hybridization between these two bands, the result is two dispersed bands with a gap in between, and hence the resulting DOS projected on the core-hole-excited atom looks just like the one we show in Fig. 3.

2. General aspects of core-hole perturbations

Having established that the main elements of the experimental results are explained by our calculations, it is interesting to try to place our work in context. It has long been suggested that there is a final state rule for core-hole band spectral *shapes* (XAS, XES, and Auger) and an initial state rule for *intensities* in spectra from simple metals.[47–51] This has been applied and tested in several cases of sp bonding, including simple metals,[50–53] silicon,[54] and graphite.[11] For Si there is little to argue against a true core-hole-induced bound state at the $L_{2,3}$ edge, or for other semiconductors and other core thresholds (see references in Ref. 54), although it has as yet not been seen as a separate spectral feature as in the case of diamond.[55,15] For simple metals like Na and Al there is little doubt that no true exciton forms, but instead a dynamic screening of the core hole leads to enhancement of the threshold intensity in both XAS and XES as a remnant ''metallic exciton.''[50] Graphite therefore appears to represent an interesting middle ground, for which no rule-of-thumb yet exists.

There are two aspects of the effect of the core hole upon which we focus: static (XDOS) and dynamic (matrix element). We have thus far concentrated on the XDOS appropriate to model XAS, and have obtained markedly improved agreement with experiment compared to a simple employment of the ground-state DOS. If one considers the screening of an electron injected into the conduction band as occurs in inverse photoemission (IPES), a quick comparison of experimental IPES data[56] (nondispersive structure at E_F+2 eV) with band structure calculations (DOS peak at E_F+2 eV in the present work vs a quasiparticle band structure[25] saddle point between 2.0 and 2.4 eV) indicates that the effect is at most minor in the present instance in line with recent measurements of quasiparticle lifetimes.[38] Thus the static effects of the core hole should dominate the shifting and shaping of the XDOS from the ground state, and the agreement between our calculations and the properly calibrated data is gratifying. The dominance of the core-hole effects is also seen for silicon.[54,57] However, for Na any static effects of the core hole near threshold are apparently hidden by dynamic effects,[58,50,59] and above threshold they seem to be completely absent, as seen in the data[58] and explained semiempirically.[50] Furthermore, for Na there is a large self-energy effect on the excited electron[60] which is quite close to what one would expect for an IPES measurement, as pointed out by Citrin *et al.*[61] Thus, for the prototypical free electron metal the core hole is screened well enough to be a relatively minor perturbation on the unoccupied states.

One feature of the XDOS which correlates well with this trend is the presence of a bound state split off from the oc-

cupied band(s). Such a bound state is apparent for Si in the results of Ma *et al.*,[54] and in the present work. For Na, this level is located at the bottom of the narrow valence band, but the core potential is unable to split it off,[50,52] although there have been claims to the contrary.[62] For a system with a gap (or with a very low value of the ground-state DOS at E_F), it is perhaps not surprising to find that screening of localized impurities is not completely effective over atomic distances. One factor which comes quickly to mind then to explain the similarity of graphite to Si in this regard is the low ground-state DOS at E_F compared to Na. Also, when we compare Na to graphite there is a difference in the wave-function overlap. For Na the *s* orbitals of one atom overlap those of many neighboring atoms, in contrast to the sp^2 covalent states of graphite, which are more spatially localized. The presence of a core hole on a Na atom contracts the wave function at this atom, but despite this the overlap with the nearest atoms is quite large. In contrast, a core hole on an atom in graphite reduces the wave-function overlap substantially, producing a perturbation of the electronic states on both the core-excited atom and nearest neighbors.

3. Spatial extent of the excitations

Another static effect which can be extracted from our results and which deserves special emphasis is the spatial extent of the perturbation produced by a 1*s* hole. Judging from the data in Fig. 2, this amounts to a radius of approximately five bond lengths for both the π^* and σ^* threshold states. Examination of Fig. 6 suggests that it is slightly larger for the π^* states. Interestingly, this is quite similar to results for, e.g., the first and strongest π^* resonance in C_{60} (see Refs. 63, 64, and, especially 65 for an image of the relevant wave function, 67a′*). It could be interesting to study the variations of this effect for systems of intermediate and smaller sizes, such as the polyacenes.[66]

4. XAS matrix elements

As pointed out in Sec. V A 2, the matrix elements which describe dynamic (screening) effects in XAS are not included in our calculations. In general, the dynamic effects in XAS of solids appear to be related to the amplitude of the DOS at E_F; in one of the earliest usages of the so-called final state rule to calculate spectra for an electron gas, one simply multiplies the ground-state DOS of a metal by a power law to simulate the dynamic enhancement (for *p* core levels) or deenhancement (for *s* core levels) of intensity at threshold.[50] Thus, for graphite one would *a priori* expect damping of the threshold intensity. However, for XES of alkali-intercalated graphite[23] a clear *enhancement* of the threshold intensity is observed. The interpretation of XAS data for *K*-intercalated graphite is less well founded, but is not inconsistent with an enhancement at threshold,[67] and there is no reason to assume that XAS and XES should be qualitatively different. We assume that this should be the case for pure graphite as well. However, there is virtually no ground-state DOS at E_F in graphite in both the ground and excited states, and this could be the reason that there is also no sign of strong intensity enhancement at threshold. Nevertheless, there has been no concensus concerning the dynamic effects in XAS, XES, and XPS, even for 3D simple metals like Na which should be ideal test cases.[62,59,68] Flynn's group attempted to isolate important influences on the XAS line shape, and derived empirical rules which suggest that the dynamical effects at threshold are maximized for cases in which the bound state lies below the band bottom, i.e., that graphite should show stronger effects than Na according to the most sophisticated calculations of the $Z+1$ DOS. This may indeed be important in explaining the alkali-intercalated graphite XES data.[23]

Finally, we point out that the present results were employed[69] to try to better understand the mechanism of resonant inelastic x-ray scattering at the π^* threshold in graphite. We note here that the these calculations indicate the important role for vibrations throughout the relevant excitation region employed in the RIXS measurements.[25,16] The width for the resonance quoted[69] was an overestimate based on smaller supercell sizes, and thus ignoring the splitting found for the larger supercells.

B. σ^* excitation

Since there is a large gap around E_F for states of σ symmetry, it is no surprise in retrospect that excitonic effects occur at the 1*s*-to-σ^* threshold.[15,17] The good agreement with experiment shown in Fig. 4 that we obtain by broadening our calculations suggests that previous interpretations[14,15,17] of the first peak as a true exciton are oversimplified, though the basic argument in terms of a symmetry gap still holds. The broader resonance above threshold is not represented at all in the calculations. This resonance is very delocalized according to resonant photoemission,[17] which agrees with the basic model employed by Batson for this region of the spectrum, except for the assumed role for core-hole effects at threshold.[14] A likely explanation for this feature is that it is a multielectron resonance. These interpretations are at odds with recent theoretical work on a series of polyacenes,[66] where it was suggested that the second resonance was likely a shape resonance.

C. Implications for C 1*s* XPS line shape and satellites

As has been noted recently[63] in calculations of the C 1*s* shake up spectrum of C_{60} and smaller aromatic molecules,[64] states which contribute to the shake up intensity are those which are most strongly perturbed by the core hole. Previous work on the shake up spectrum of graphite concluded[19,20] that a ground-state-like DOS profile for the occupied states, coupled with a tailored version of the measured[11] unoccupied XDOS, could explain the measured metallic C 1*s* XPS profile for graphite. It was suggested by Enkvist *et al.* that this was an oversimplification due to the likely perturbations of the occupied states by the core hole,[63] which is supported by the strong changes obtained in the present calculations. Most important is that there are quite nonuniform alterations of the DOS by the excitation, indicating clearly the need for explicit consideration of the matrix elements in calculations of core level shake up of graphite.

VI. SUMMARY

In summary, we have obtained a good agreement between theoretical and experimental data for the π^* and σ^* reso-

nances in graphite. The total lack of agreement between theory and experiment for the second σ^* resonance points to an important role for multielectron excitations. Our theoretical calculations show that the presence of the core hole must be considered in order to reproduce experiment. Thus, we come to the conclusion, as did[11] Mele and Ritsko, that the π^* resonance in graphite is to be associated with a Frenkel exciton. The exciton is mostly localized on the core-excited atom, but there is also some weight at the nearest-neighbor atoms. This is most easily detected from the projected DOS of the different atoms in the supercell, which show that the nearest-neighbor atoms and also to some extent the next-nearest atoms have a redistribution of the DOS when the core electron is excited. We also find that the occupied electronic states are strongly modified when the core hole is excited. To be specific, the core-hole-excitation results in a narrow s peak at E_F-19 eV and a smaller feature at E_F-7 eV.

The magnitude of the broadening found for the π^* resonance cannot be explained here quantitatively, but as noted above is of the same magnitude as found in benzene. This we attribute to vibronic effects.

In addition, other fine details in the absorption spectra elude an explanation at this point. We have not calculated the matrix elements, which could well contribute effects of the order of the discrepancies shown in Figs. 3 and 4 for excitation above the primary resonances, for both the π^* and σ^* thresholds. E.g., multielectron excitations could contribute significantly to the spectra over a wide range. Future improvements on the theory of graphite 1s threshold absorption might be obtainable along the lines of recent calculations for metals.[70]

Note added in proof. We came upon published XES data which substantiate in large measure the present results for the effect of a core hole on the local occupied DOS.[71] The double-core-hole satellite data shown there give a clear indication of the peak at E_F-7 eV in Fig. 5, and verify its location. Mansour, Schnatterly, and Carson anticipated some of the results here regarding excitonic effects as well.[71]

ACKNOWLEDGMENTS

The authors are grateful to the Swedish Natural Science Research Foundation (NFR) for financial support. Part of these calculations were done at the National Supercomputer Center (NSC) in Linköping. Support from the Swedish Materials Research Consortia on Theoretical and Computational Materials Physics, and on Clusters and Ultrafine Particles, which are funded by NFR and NUTEK, the Swedish Board for Industrial and Technical Development, is appreciated.

[1] J. W. McClure, Phys. Rev. **108**, 612 (1957).
[2] J. C. Slonczewski and P. R. Weiss, Phys. Rev. **109**, 272 (1958).
[3] A. Zunger, Phys. Rev. B **17**, 626 (1978).
[4] R. C. Tatar and S. Rabii, Phys. Rev. B **25**, 4126 (1982).
[5] H. J. F. Jansen and A. J. Freeman, Phys. Rev. B **35**, 8207 (1987).
[6] D. A. Fisher, R. M. Wentzcovitch, R. G. Carr, A. Continenza, and A. J. Freeman, Phys. Rev. B **44**, 1427 (1991).
[7] N. A. W. Holzwarth, S. G. Louie, and S. Rabii, Phys. Rev. B **26**, 5382 (1982).
[8] J.-C. Charlier, X. Gonze, and J.-P. Michenaud, Phys. Rev. B **43**, 4579 (1991).
[9] M. C. Schabel and J. L. Martins, Phys. Rev. B **46**, 7185 (1992).
[10] R. Ahuja *et al.*, Phys. Rev. B **51**, 4813 (1995).
[11] E. J. Mele and J. J. Ritsko, Phys. Rev. Lett. **43**, 68 (1979).
[12] R. A. Rosenberg, P. J. Love, and V. Rehn, Phys. Rev. B **33**, 4034 (1986).
[13] L. J. Terminello *et al.*, Chem. Phys. Lett. **182**, 491 (1991).
[14] P. E. Batson, Phys. Rev. B **48**, 2608 (1993).
[15] Y. Ma *et al.*, Phys. Rev. Lett. **71**, 3725 (1993).
[16] P. Skytt *et al.*, Phys. Rev. B **50**, 10 457 (1994).
[17] P. A. Brühwiler *et al.*, Phys. Rev. Lett. **74**, 614 (1995).
[18] F. R. McFeely *et al.*, Phys. Rev. B **9**, 5268 (1974).
[19] P. M. T. M. van Attekum and G. K. Wertheim, Phys. Rev. Lett. **43**, 1896 (1979).
[20] F. Sette *et al.*, Phys. Rev. B **41**, 9766 (1990).
[21] J. E. Houston *et al.*, Phys. Rev. Lett. **56**, 1302 (1986); Phys. Rev. B **34**, 1215 (1986).
[22] G. M. Mikhailov *et al.*, J. Electron Spectrosc. Relat. Phenom. **46**, 145 (1988).
[23] A. Mansour, S. E. Schnatterly, and J. J. Ritsko, Phys. Rev. Lett. **58**, 614 (1987).
[24] A. Šimůnek and G. Wiech, Phys. Rev. Lett. **61**, 1140 (1988).
[25] J. A. Carlisle *et al.*, Phys. Rev. Lett. **74**, 1234 (1995).
[26] X. Weng, P. Rez, and H. Ma, Phys. Rev. B **40**, 4175 (1989).
[27] Y. Zou and J. C. Tang, J. Phys. Condens. Matter **6**, 2949 (1994).
[28] R. V. Vedrinskii *et al.*, J. Phys. Condens. Matter **6**, 11 045 (1994).
[29] J. M. Wills (unpublished); J. M. Wills and B. R. Cooper, Phys. Rev. B **36**, 3809 (1987); D. L. Price and B. R. Cooper, *ibid.* **39**, 4945 (1989).
[30] O. K. Andersen, Phys. Rev. B **12**, 3060 (1975).
[31] H. L. Skriver, *The LMTO Method* (Springer, Berlin, 1984).
[32] S. C. Erwin and W. E. Pickett, Phys. Rev. B **42**, 11 056 (1990).
[33] V. A. Beryazov and R. A. Evarestov, Teor. Éksp. Khim. **26**, 63 (1990).
[34] D. J. Chadi and M. L. Cohen, Phys. Rev. B **8**, 5747 (1973); S. Froyen, *ibid.* **39**, 3168 (1989).
[35] L. Hedin and B. I. Lundqvist, J. Phys. C **4**, 2064 (1971).
[36] M. Vračko, C.-M. Liegener, and J. Ladik, Chem. Phys. Lett. **153**, 166 (1988).
[37] The width for the ground-state DOS singularity in the tight-binding calculations of Mele and Ritsko (Ref. 11) is open to interpretation, since the peak merges continuously into the sloping DOS towards E_F.
[38] S. Xu *et al.*, Phys. Rev. Lett. **76**, 483 (1996).
[39] P. A. Brühwiler *et al.*, Phys. Rev. Lett. **71**, 3721 (1993).
[40] S. J. Osborne *et al.*, J. Chem. Phys. **102**, 7317 (1995), recently presented data for the lifetime broadening of the C 1s level determined from XAS and XPS of CO in the gas phase. These data indicate that correlations among the valence electrons in the core-excited state act to minimize the interaction between the excited electron in the π^* resonance and the core hole, thus yielding a longer core-hole lifetime than for ionized CO, contrary to the assumptions employed in Refs. 39 and 17. On the

other hand, the difference between the two situations was not a large percentage of the total width, thus lending support to our order-of-magnitude estimates.

[41] Y. Ma *et al.*, Phys. Rev. Lett. **63**, 2044 (1989).

[42] W. A. Harrison, *Electronic Structure and the Properties of Solids* (Freeman, San Francisco, 1980).

[43] E. Rotenberg *et al.*, Phys. Rev. B **54**, R5279 (1996).

[44] C. Pisani, R. Dovesi, and P. Carosso, Phys. Rev. B **20**, 5345 (1979).

[45] One can estimate an upper limit on the hopping contribution to the width of the π^* resonance as described in Ref. 17. Those workers estimated the resonant photoemission contribution to the total intensity starting with a 20% contribution from the excited electron, assuming it to be totally localized to the excited atom; this should be changed to 1/6 since the core-hole site is almost completely screened even without the excited electron. If one then takes the difference spectrum defined by the data shown in Fig. 3 of Ref. 17 as the single-hole contribution, its area is about 8% of the total. An upper limit on the intrinsic electronic width of the π^* resonance is then given by $\Delta=(1/6)(0.1\ \text{eV})/(0.08)=0.21$ eV, which is of the same order of magnitude as that found here theoretically. This estimate would clearly not work for the same normalization procedure at the σ^* threshold, and thus must be considered suspect as a measure of the hopping. An intensity calibration might resolve this issue through avoidance of the semiarbitrary normalization procedure used there. Other difficulties with this approach are the neglect of specific excited-state valence electron correlations, such as discussed in Ref. 40.

[46] P. A. Brühwiler *et al.*, Chem. Phys. Lett. **193**, 311 (1992).

[47] V. I. Grebennikov, Y. A. Babanov, and O. B. Sokolov, Phys. Status Solidi B **80**, 73 (1977).

[48] U. von Barth and G. Grossmann, Solid State Commun. **32**, 645 (1979).

[49] G. D. Mahan, Phys. Rev. B **21**, 1421 (1980).

[50] U. von Barth and G. Grossmann, Phys. Scr. **28**, 107 (1983).

[51] P. Livins and S. E. Schnatterly, Phys. Rev. B **37**, 6731 (1988).

[52] W. Speier, J. F. van Acker, and R. Zeller, Phys. Rev. B **41**, 2753 (1990).

[53] J. F. van Acker, W. Speier, J. C. Fuggle, and R. Zeller, Phys. Rev. B **43**, 13 916 (1991).

[54] H. Ma, S. H. Lin, R. W. Carpenter, and O. F. Sankey, Phys. Rev. B **44**, 13 393 (1991).

[55] J. F. Morar *et al.*, Phys. Rev. Lett. **54**, 1960 (1985).

[56] H. Ohsawa *et al.*, Solid State Commun. **61**, 347 (1987).

[57] We note that Ma *et al.* (Ref. 54) conclude that even in XAS it is appropriate to use ground-state (''unrelaxed'') wave-functions for the occupied states in Si in the presence of a $2p$ hole. This is due to the possibility found there to use such wave functions to describe the Si XES DOS. However, this latter is consistent with the final state rule (Refs. 47–51), and thus says little directly about the rate of valence relaxation in the presence of a core hole.

[58] T. A. Callcott, E. T. Arakawa, and D. L. Ederer, Phys. Rev. B **18**, 6622 (1978).

[59] P. A. Brühwiler and S. E. Schnatterly, Phys. Rev. B **41**, 8013 (1990); **42**, 9713(E) (1990).

[60] See, e.g., Fig. 8 of Ref. 58.

[61] P. H. Citrin *et al.*, Phys. Rev. Lett. **61**, 1021 (1988).

[62] T.-H. Chiu, D. Gibbs, J. E. Cunningham, and C. P. Flynn, Phys. Rev. B **32**, 588 (1985).

[63] C. Enkvist *et al.*, Phys. Rev. B **48**, 14 629 (1993).

[64] C. Enkvist *et al.*, J. Chem. Phys. **103**, 6333 (1995).

[65] S. Lunell *et al.*, Int. J. Quantum. Chem. **52**, 135 (1994).

[66] H. Ågren, O. Vahtras, and V. Carravetta, Chem. Phys. **196**, 47 (1995).

[67] J. J. Ritsko, Phys. Rev. B **25**, 6452 (1982).

[68] E. Zaremba and K. Sturm, Phys. Rev. Lett. **66**, 2144 (1991).

[69] P. A. Brühwiler *et al.*, Phys. Rev. Lett. **76**, 1761 (1996).

[70] E. Tamura, J. van Ek, M. Fröba, and J. Wong, Phys. Rev. Lett. **74**, 4899 (1995).

[71] A. Mansour, S. E. Schnatterly, and R. D. Carson, Phys. Rev. B **31**, 6521 (1985).